Tampere University

Tiina Jäntti

CHARACTERIZATION OF IMMUNE CELL INFILTRATION IN HIGH-GRADE SEROUS OVARIAN CARCINOMA

Faculty of Medicine and Health Technology
Thesis of Advanced Studies
June 2020

TIIVISTELMÄ

Tiina Jäntti: IMMUUNISOLUJEN INFILTRAATION KARAKTERISOINTI HUONOSTI ERILAISTUNEESSA SEROOSISSA MUNASARJASYÖVÄSSÄ
Syventävien opintojen opinnäytetyö
Tampereen yliopisto
Lääketieteen lisensiaatin tutkinto-ohjelma
Kesäkuu 2020
Alkuperäinen artikkeli: Characterization of immunoreactivity with whole slide imaging and digital analysis in high-grade ovarian carcinoma. Tekijät: Tiina Jäntti[1], Satu Luhtala[1], Johanna Mäenpää, Synnöve Staff.
[1]Tasavertainen työpanos.

Munasarjasyöpä on gynekologisista syövistä huonoennusteisin. Huonosti erilaistunut seroosi karsinooma *(high-grade serous carcinoma,* HGSC) on munasarjasyövän yleisin histologinen alatyyppi, jolle on tyypillistä aggressiivinen levittäytyminen. Munasarjasyöpäpotilaiden viiden vuoden elossaololuku on vain noin 45 %. Ennustetta huonontavat myöhäinen diagnosointi, mikä johtuu spesifisten oireiden ja toimivien seulontamenetelmien puutteesta, sekä hoitoresistenssin kehittyminen. Siksi uusia hoitomuotoja, kuten immuno-onkologisia hoitoja, tarvitaan. Tuumorin mikroympäristön (*tumor microenvironment*, TME) ja siinä esiintyvien immuunisolujen toiminnan tunteminen on tärkeää immuno-onkologisten hoitojen kehittämiseksi ja hoidosta hyötyvien potilaiden tunnistamiseksi. Digitaalisilla kuva-analyysimenetelmillä (*digital image analysis,* DIA) voidaan lisätä TME:n immuunisolujen määrityksen luotettavuutta ja toistettavuutta.

Tämän tutkimuksen tarkoituksena oli selvittää immuunisolujen ilmentymistä HGSC-kudoksen TME:ssä retrospektiivisestä potilaskohortista hyödyntäen virtuaalimikroskopiaa (*whole slide imaging*, WSI) ja digitaalista kuva-analyysiä.

Tutkimusaineisto koostui Tampereen yliopistollisessa sairaalassa (Tays) 2001–2013 leikattujen HGSC-potilaiden (n=67) kasvainnäytteistä (formaliinifiksoidut, parafiinipedatut FFPE-blokit). Tuumorinäytteille on tehty seuraavat immunohistokemialliset värjäykset tunnistaen erilaisia TME:n immuunisoluja: CD4 (auttaja-T-lymfosyytit), CD8 (tappaja-T-lymfosyytit), FoxP3 (säätelijä-T-lymfosyytit), grantsyymi B (aktivoituneet lymfosyytit ja luonnolliset tappajasolut), CD68 (M1- ja M2-makrofagit) ja CD163 (M2-makrofagit). Värjäykset on analysoitu digitaalisesti QuPath 0.1.2- ja ImageJ-ohjelmilla ja tulokset on yhdistetty potilasasiakirjoista kerättyihin, kliinispatologisiin tietoihin.

Tutkimuksessa CD8-, grantsyymi B- ja CD163-positiivisten solujen suuremmat määrät tuumorikudoksessa olivat yhteydessä pidempään tautivapaaseen aikaan (*progression free survival*, PFS). Kuitenkin vain sekä CD8- että grantsyymi B -solujen yhtäaikainen suurempi määrä oli yhteydessä pidempään PFS:iin monimuuttuja-analyysissa (HR=0,287; p=0,002). Lisäksi neoadjuvanttikemoterapian (*neoadjuvant chemoterapy*, NACT; ennen leikkausta annettu sytostaattihoito) jälkeen otetuissa näytteissä FoxP3+ solujen määrä oli pienempi kuin ennen hoitoa otetuissa tai primaarileikattujen potilaiden näytteissä (Fisherin tarkka testi; p=0,013).

CD8- ja grantsyymi B -solujen yhtäaikainen ilmentyminen tuumorikudoksessa oli yhteydessä munasarjasyövän parempaan ennusteeseen viitaten mahdollisesti TME:n aktivoituneeseen, syövänvastaiseen immuunivasteeseen. NACT voi vaikuttaa TME:n immuunisolujen jakaumaan ja näin ollen kemoterapian ja immuno-onkologisten hoitojen tehoon.

Asiasanat: ovariokarsinooma, immunoreaktiivisuus, immuno-onkologia, tuumorin mikroympäristö, digitaalinen kuva-analyysi
Tämän julkaisun alkuperäisyys on tarkastettu Turnitin OriginalityCheck –ohjelmalla.

CONTENTS

1 ABSTRACT

1.1 Objectives

Ovarian cancer (OC) is the most lethal of gynecological cancers with five-year survival rate of only ca. 45 %. The most common histologic subtype is high-grade serous carcinoma (HGSC), which typically is presented with advanced stage and development of chemoresistance. Therefore, new treatment options, including immunotherapies, are needed. Understanding the features of the immune cell populations and their interaction in the tumor microenvironment (TME) is essential for developing personalized treatment options and finding predictive biomarkers. Digital image analysis (DIA) may enhance the accuracy and reliability of immune cell infiltration assessment in the TME.

The aim of this study was to characterize TME in a retrospective cohort of high-grade serous ovarian cancer samples with whole-slide imaging (WSI) and digital image analysis (DIA).

1.2 Methods

Formalin-fixed paraffin-embedded (FFPE) HGSC tumor tissue samples (n=67) were analyzed for six different immunohistochemical (IHC) stainings: CD4, CD8, FoxP3, granzyme B, CD68 and CD163. The stained sample slides were scanned into a digital format and assessed using QuPath 0.1.2. and ImageJ softwares. Staining patterns were associated with clinicopathological data.

1.3 Results

The higher numbers of CD8+, CD163+ and granzyme B+ immune cells were associated with survival benefit when analyzed individually, while high levels of both CD8+ and granzyme B+ tumor-infiltrating lymphocytes (TILs) was an independent prognostic factor in Cox multivariate regression analysis (median PFS; HR=0.287, p=0.002). In addition, the given neoadjuvant

chemotherapy (NACT) was associated with lower FoxP3+ TIL density (Fisher's exact test, p=0.013).

1.4 Conclusions

Tumors having high amount of both CD8+ and granzyme B+ TILs showed better prognosis, possibly reflecting an activated immune state in the TME. The combined positivity of CD8 and granzyme B warrants further investigation with respect to predicting response to immune therapy. NACT may have an effect on the TME and therefore on the response to immuno-oncologic or chemotherapy treatments.

2 INTRODUCTION

Ovarian cancer (OC) is the third most common and the most lethal gynecological cancer (1). High-grade serous carcinoma (HGSC) is the most common histological subtype, characterized by aggressive dissemination (2,3). The standard treatment of OC is primary cytoreductive (debulking) surgery (PDS), followed by platinum-based combination chemotherapy with or without bevacizumab (4-6). In some cases with advanced disease, neoadjuvant chemotherapy (NACT) and interval debulking surgery (IDS) may be considered (4,7,8). The poor prognosis in OC (five-year survival ca 45 %) is caused by late diagnosis (67–75 % at FIGO III–IV) due to lack of specific symptoms and screening methods and by the development of chemoresistance over cumulative treatment lines (2,4). Most of the patients respond to primary treatment. However, nearly 80 % of patients with advanced disease will relapse and recurrence is mostly incurable. (4) Despite the recent paradigm shift in front-line OC treatment with PARP inhibitors (9-11), there is still urgent need for new OC treatment options, including immunotherapies. Immune cells and immunoregulatory molecules present in the tumor microenvironment (TME) are involved both in anti-tumor immune responses of the host and in immunosuppressive mechanisms promoting cancer progression. Understanding the nature and characteristics of TME is essential for developing immuno-oncologic treatment options and discovering predictive biomarkers for patient selection. (12-14)

Tumor-infiltrating lymphocytes (TILs) infiltrate to the tumor epithelium (intraepithelial, ieTILs) or locate at the peritumoral stroma (stromal, sTILs) (15). Intraepithelial CD3+ TILs (T cells) have been associated with improved patient outcome in OC (16-21). When assessing the subsets of T cells, particularly CD8+ TILs (cytotoxic T-lymphocytes, Tc or CTL) (17-20,22-26), and, in some studies, CD4+ TILs (T helper, Th) (22) have been associated with favourable prognosis. Activated CTLs and natural killer (NK) cells eliminate cancer cells by secreting cytolytic enzymes, including granzyme B (27).

FoxP3+ regulatory T cells (Tregs) may in turn suppress anti-tumor immunity (15). The reports of impact of Tregs on prognosis of OC or other cancers

have been contradictory (18,19,24,28-30). Tumor-associated macrophages (TAMs) are further divided into M1 and M2 subtypes, of which M1 TAMs contribute to elimination of cancer cells, whereas anti-inflammatory M2 type is involved with tissue repair, angiogenesis and cancer progression (31). There is no clear consensus on the role of M1 and M2 type of TAMs in OC, but according to available data, CD68+ (M1 and M2) TAM density may not act as prognostic factor (19,21,32-34).

In addition, administration of NACT may alter the immune cell populations in TME. Although previously considered immunosuppressive, NACT has more recently been found to have anti-tumor immunity enhancing effects. (35) However, results considering the impact of NACT on the immune cells in OC TME and the prognostic significance of post-NACT TILs have been highly variable (20,25,30,36,37). Immune cell infiltration in OC has been studied extensively, yet results considering the prognostic significance of immune cells in the TME are highly variable (15,18). Currently, there are no established cut-off values or analyzing methods for assessment of TILs, which may weaken the reproducibility of the studies. The use of whole slide imaging (WSI) and digital image analysis (DIA) has been found to increase the reliability and accuracy of assessment of immune cells when compared to manual analysis and semi-quantitative scales (38,39). Therefore, the present study focusing on HGSC was set up to clarify, which immune cells or biomarkers present in TME are associated with clinical outcome. For optimal accuracy, WSI and DIA were used in the analyses.

3 MATERIALS AND METHODS

3.1 Patients and samples

The study was carried out at the Tampere University Hospital (TAUH) and the Faculty of Medicine and Health Technology, University of Tampere, Tampere, Finland. The study protocols have been approved by the Regional Ethics Committee of the Expert Responsibility area of Tampere University Hospital (identification codes: ETL-R09108 and ETL-R11137). All the study patients have provided a signed informed consent.

The present retrospective study cohort is consisted of tumor samples from two different cohorts of epithelial ovarian cancer (EOC) patients who had undergone primary or interval debulking surgery in TAUH during 2001–2009 and 2011–2013. Patients were recruited to the study when they were being treated with chemotherapy in either adjuvant or recurrent setting (older surgery cohort of 2001–2009) or when they have been scheduled for EOC surgery (surgery cohort of 2011–2013). The morphological and histological findings from the available and representative archival surgical tumor specimens were assessed by experienced pathologists at the Department of Pathology of TAUH. Only samples from patients with histologically verified high-grade ovarian cancer were included in the final study cohort, which consisted of 67 high-grade ovarian cancer samples having sufficient tumor tissue content and technical quality for analyses.

Clinical, pathological and follow-up data were collected from the patient records. As the patients were operated prior to 2014, the staging was adjusted to the FIGO 2014 staging classification. Surgical outcome was classified as following: R0 = no macroscopic residual tumor, R1 = residual tumor < 1 cm, R2 = residual tumor > 1 cm. Median age at diagnosis was 63 years (range 38–78). Almost all patients (n=64; 96 %) had verified HGSC histology. Most of the patients (n=60; 90 %) presented with an advanced stage disease (FIGO III/IV) with a median OS of 52 months (range 11–163) and PFS of 16 months (range 5–124). The main clinico-pathological characteristics of the study patients are summarized in Table 1.

3.2 Immunohistochemical stainings and interpretation

The HGSC tissue samples were formalin-fixed and paraffin-embedded (FFPE) prior to immunohistochemical (IHC) stainings. FFPE samples were cut into 3–4 µm thick sequential sections that were then baked, deparaffinized and pretreated by boiling them in Tris-EDTA buffer (pH 9) at + 98 °C for 15 minutes for epitope retrieval. Immunohistochemical stainings were performed by indirect HRP-based detection technique. Six IHC stainings were performed: CD4, CD8, FoxP3, granzyme B, CD68 and CD163. The antibodies, clones and used dilutions are presented in Table 2. The tissue sections were counterstained with Mayer's hematoxylin (Oy FFChemicals Ab, Haukipudas, Finland) to give contrast for positive staining reaction visualized as brown DAB precipitate. Staining protocols were carried out with Autostainer 480 (Lab Vision, CA, USA) automated immunostainer.

The stained sample slides were scanned into a digital format by using Hamamatsu NanoZoomer S60 Digital Slide Scanner. The digital whole slide images (WSI) were analyzed using QuPath 0.1.2. DIA software (40). Three hot spot areas of 1 mm² tumor tissue were selected from each slide. For CD4, CD8, FoxP3 and granzyme B stainings, the positively stained intraepithelial immune cells in each 1 mm² area were counted digitally by using QuPath. For optimal accuracy, the cell counts were occasionally revised manually. For CD68 and CD163 stainings, the hot spot areas were selected using QuPath and the percentages of positively stained areas were calculated by using ImageJ (41). The mean cell count or positively stained proportion of the three selected hot spots was calculated for each image. The above-mentioned analyses were performed separately by an experienced cell biologist (SL) and the first author (TJ). The mean of the obtained results was used for statistical analyses. Any discrepancies between the analyses were discussed until a consensus was achieved.

3.3 Statistical analyses

Statistical analyses were performed using IBM SPSS Statistics 25.0 software. Progression free survival (PFS) was defined as time from diagnosis to the first recurrence. Overall survival (OS) was defined as time from diagnosis to death. Data were censored to the last follow-up for patients that were alive and/or had no recurrence at the time of data collection.

Kolmogorov-Smirnov test and Shapiro-Wilk tests were used for determining the normality of the variable distributions. Medians of cell densities or areas stained / 1mm² tumor tissue were compared between groups using Mann-Whitney U-test. Chi-square test and Fisher's exact test were used when comparing log transformed cell densities or areas stained as dichotomous variables. Kaplan-Meier method was used for analyzing cumulative survival, and differences in survival between groups were compared by log-rank test. A cut-off value for cell densities or areas stained was set at the lowest 10^{th} percentile. Hazard ratios (HR) and 95 % confidence intervals (CI) were analyzed by Cox proportional hazards regression model. Cell densities or areas stained / 1 mm² tumor tissue were log transformed when analyzed as continuous variables in regression models. Cell densities that showed a significant correlation with survival in univariate Cox regression analysis, were entered to a multivariate analysis with known prognostic factors: size of residual tumor after surgery (R0 or R1/R2), NACT and stage at diagnosis (FIGO I/II or III/IV). P-value ≤ 0.05 was considered statistically significant.

Table 1: Patient characteristics

	Total (n=67)	
Age at diagnosis (y); median (range)	63	(38–80)
Stage at diagnosis; n (%)		
I	1	(1.5)
IIA/IIB	6	(9.0)
IIIA/IIIB	3	(4.5)
IIIC	41	(61.2)
IVA/IVB	16	(23.9)
Grade; n (%)		
1–2	0	(0.0)
3	67	(100.0)
Histology; n (%)		
Serous	63	(94.0)
Transitional cell	1	(1.5)
Other or undefined epithelial	3	(4.5)
Ca 12-5 prior to treatment (kU/l); median (range)	719	(11–8909)
Ca 12-5 after treatment (kU/l); median (range)	16	(5–904)
BRCA status; n (%)		
Wild type	7	(10.4)
BRCA1	0	(0)
BRCA2	3	(4.5)
Not tested	57	(85.1)
Anti-inflammatory medication; n (%)		
Yes	4	(6.0)
No	63	(94.0)
Other cancers, n (%)		
Yes, breast	4	(6.0)
Yes, other than breast	4	(6.0)
No	59	(88.1)
Residual disease; n (%)		
R0	16	(23.9)
R1	12	(17.9)
R2	39	(58.2)
First-line chemotherapy; n (%)		
Paclitaxel-carboplatin	23	(34.3)
Paclitaxel-carboplatin-bevacizumab	11	(16.4)
Paclitaxel-carboplatin, switched to another platinum-based during first-line treatment	27	(40.3)
Other platinum-based	6	(9.0)
First-line chemotherapy cycles; median (range)	6	(4–18)
Neoadjuvant chemotherapy; n (%)		
Yes	15	(22.4)
No	52	(77.6)

Overall survival (m); median (range)	52	(11–163)
Progression free survival (m); median (range)	16	(5–124)
Platinum free interval (m); median (range)	10	(0–120)
Alive; n (%)		
Yes	14	(20.9)
No	53	(79.1)
Recurrence; n (%)		
Platinum sensitive (complete, 12 m) at first recurrence	22	(34.3)
Platinum sensitive (partial, 6–12 m) at first recurrence	16	(23.9)
Platinum resistant at first recurrence	21	(31.3)
No recurrence	8	(11.9)

Table 2
Antibodies used for immunohistochemical stainings

Antibody	Detectable cells	Clone	Host species	Manufacturer	Dilution
FoxP3	Tregs	236A/E7	Mouse mAb	Abcam	1:100
Granzyme B	activated lymphocytes and NK cells	BSR150	Rabbit mAb	Nordic Biosite	1:300
CD4	Th	BSR4	Rabbit mAb	Nordic Biosite	1:300
CD8	Tc (CTL)	BSR5	Rabbit mAb	Nordic Biosite	1:200
CD68	M1 and M2 macrophages	KP1	Mouse mAb	Zeta Corporation	1:1200
CD163	M2 macrophages	Ed-Hu1	Mouse mAb	Bio-Rad	1:700

Abbreviation: mAb = monoclonal antibody.

4 RESULTS

The final study cohort consisted of 67 high-grade ovarian cancer samples. The sample topography is presented in Table 3. Most of the analyzed samples originated from the adnexa (89.6 %). High individual variation in the densities of CD4+ (0–2416), CD8+ (1–4020) and granzyme B+ cells (3–3028) was observed. Median cell densities (CD4+, CD8+, FoxP3+ and granzyme B+) or positively stained areas (CD68+ and CD163+) are summarized in Table 4 and examples of immunostainings are presented in Figure 1. A correlation between prolonged median PFS (17.00 vs 9.00 months for all comparisons) and higher combined CD8+ and granzyme B+ (p=0.003), granzyme B+ (p=0.002), CD8+ (p=0.018) and CD163+ (p=0.004) cell densities was observed in Kaplan-Meier analysis (Figure 2). The higher number of granzyme B+ cells was correlated with prolonged median PFS also in univariate Cox proportional hazard regression (HR=0.820, p=0.032; Table 5) but only the combined higher amount of both CD8+ and granzyme B+ cells was correlated with prolonged median PFS both in univariate (HR=0.334, p=0.006) and multivariate (HR=0.287, p=0.002) Cox regression analysis (Table 5). None of the studied immunomarkers was associated with OS (data not shown) or with clinical factors (data not shown).

Post-NACT tumor samples (n=7) presented with lower densities of FoxP3+ cells (Figure 1 K–L; cut-off 10^{th} percentile (9 cells / mm^2), Fisher's exact test, p=0.013). The median densities of CD4+ and granzyme B+ TILs were more than 50 % lower in post-NACT samples, but the differences between groups were not statistically significant (data not shown).

Table 3
Sample topography

	Total (n=67)	
	n	(%)
Ovary	45	(67.2)
Fallopian tube	5	(7.5)
Adnexa (not otherwise specified)	10	(14.9)
Uterine serosa, tubal serosa	1	(1.5)
Omentum	2	(3.0)
Peritoneum	1	(1.5)
Sigmoid colon	1	(1.5)
Topography unknown	2	(3.0)

Table 4
Cell densities[1] or percentages of areas stained[2] / 1 mm² tumor tissue; median (range)

	Median	(Range)
FoxP3[1]	99	(0–497)
Granzyme B[1]	238	(3–3028)
CD4[1]	180	(0–2416)
CD8[1]	328	(1–4020)
CD68[2]	12	(2–43)
CD163[2]	10	(0–35)

Table 5

Cox proportional hazards regression

	Univariate			Multivariate		
	Exp (B)	95 % CI	p	Exp (B)	95 % CI	p
NACT						
no	reference			reference		
yes	2.682	1.447–4.973	0.002	2.275	1.438–5.165	0.002
Optimal cytoreduction						
no (R1/R2)	reference			reference		
yes (R0)	0.409	0.209–0.798	0.009	0.369	0.183–0.744	0.005
Stage						
I/II	reference			reference		
III/IV	3.588	1.111–11.590	0.033	2.045	0.606–6.900	0.249
Age	1.002	0.973–1.033	0.886			
FoxP3	0.908	0.748–1.101	0.327			
Granzyme B	0.820	0.684–0.984	0.032			
CD4	0.993	0.855–1.154	0.932			
CD8	0.934	0.794–1.098	0.406			
CD68	0.914	0.550–1.521	0.730			
CD163	0.719	0.475–1.088	0.118			
CD8+ and granzyme B+						
no	reference			reference		
yes	0.334	0.153–0.730	0.006	0.287	0.127–0.648	0.003

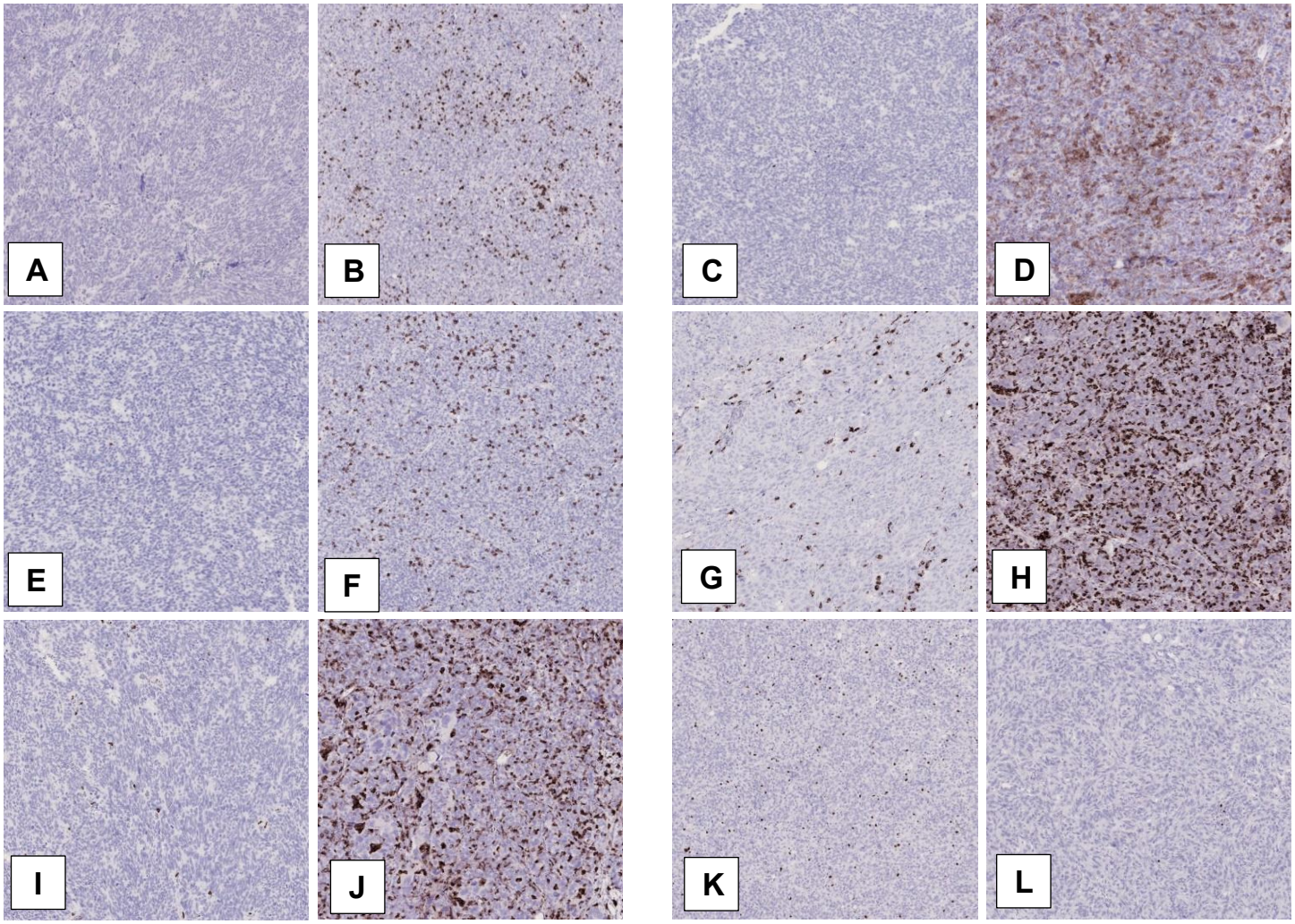

Figure 1. Examples of immunostaining patterns.
Granzyme B staining , low (5 positive cells / mm^2, **A**) and high (1312 positive cells / mm^2, **B**); CD4 staining, low (4 positive cells / mm^2, **C**) and high (1438 positive cells / mm^2, **D**); CD8 staining, low (2 positive cells / mm^2, **E**) and high (926 positive cells / mm^2, **F**); CD68 staining, low (positively stained area 4 %, **G**) and high (positively stained area 25 %), CD163 staining, low (positively stained area 1 %, **I**) and high (positively stained area 20%, **J**); FoxP3 staining, high (207 positive cells / mm^2, treatment naïve, **K**) and low (7 positive cells / mm^2, NACT treated, **L**).

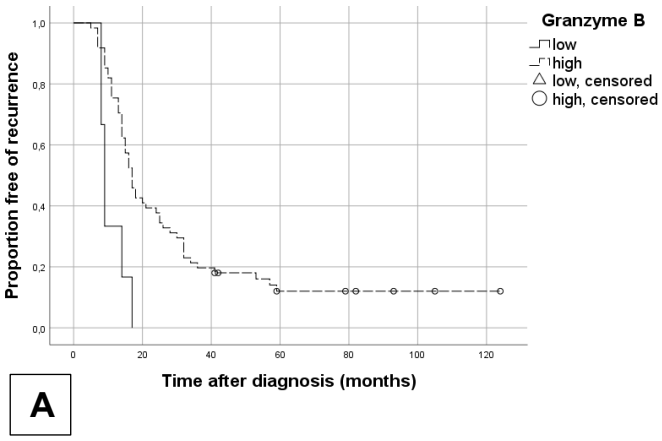

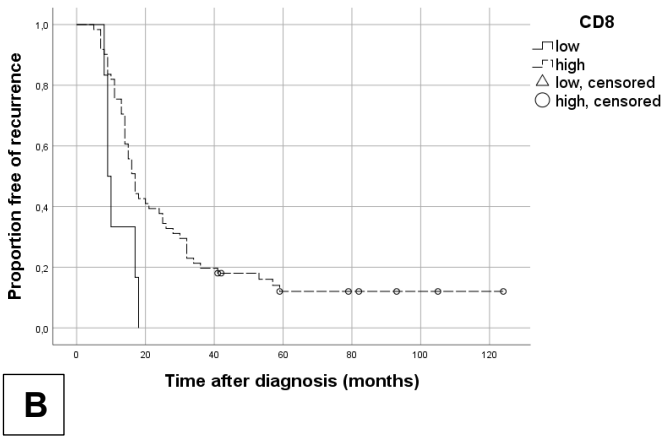

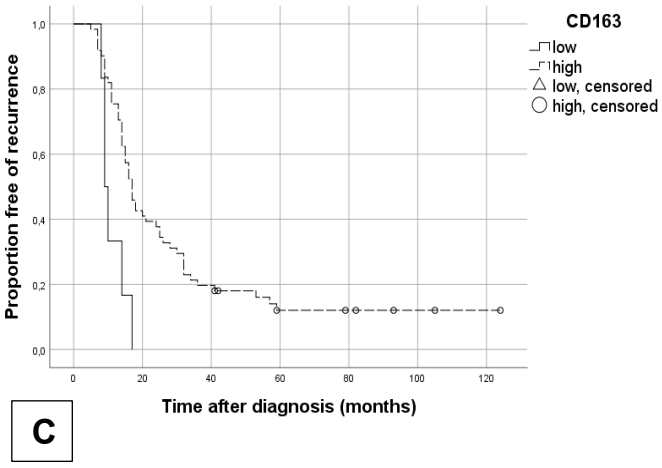

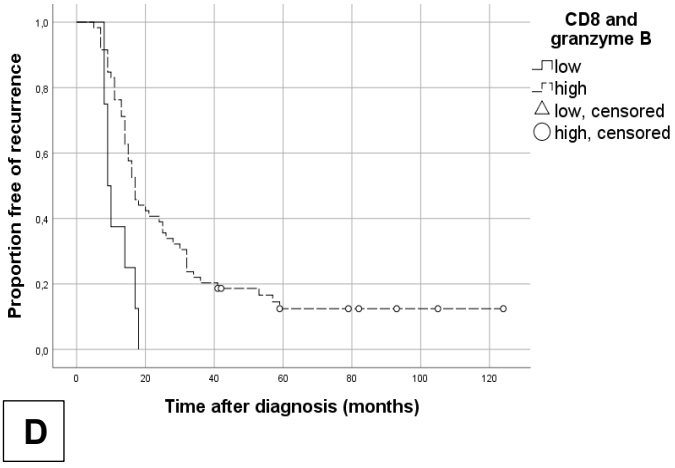

Figure 2. Kaplan-Meier analyses.
A) Granzyme B; cut-off 10th percentile (16 cells / mm^2). Log-rank p=0.002. **B)** CD8; cut-off 10th percentile (28 cells / mm^2). Log-rank p=0.018. **C)** CD163; cut-off 10th percentile (3 %/mm^2). Log-rank p=0.004. **D)** CD8; cut-off 10th percentile (28 cells / mm^2) and granzyme B: cut-off 10th percentile (16 cells / mm^2). Log-rank p=0.003.

5 DISCUSSION

Here, we report the results of characterization of various TME immunomarkers in a cohort of high-grade serous ovarian cancer patients. According to our results, combined high CD8 and granzyme B expression correlated with prolonged PFS. Granzyme B is considered as the most important cytolytic enzyme by which activated NK cells and CD8+ TILs destroy tumor cells (27). The prognostic benefit of CD8+ TILs has been previously shown in many studies (17-20,22-26). However, the association of CD8+ TILs with improved survival has not been systematically shown in OC throughout all patient subgroups (25,30). The higher amount of positive CD8 and granzyme B cells showed statistical significance with longer PFS in multivariate analysis in the present study. This might imply that activated NKs and CTLs or other TILs confer the immunogenic phenotype associated with improved survival and that the activation status of CTLs may be as important as the cell density or even more important (27,30). Previously, Milne et al. (19) found that granzyme B infiltrates were highly correlated with CD8 TILs while the expression of NK cell markers was low, indicating that granzyme B is mostly expressed by T cells in the TME of HGSC and therefore the combined positivity of both CD8 and granzyme B may represent a surrogate marker of activated immune state in the TME. Previously, there has been relatively little data considering the granzyme B expression, or simultaneous expression of CD8 and granzyme B in the TME and OC prognosis, and therefore the results reported here make a valuable addition to the existing data. It has been shown that higher post-chemotherapy granzyme B+ / FoxP3+ cell ratio was associated with better prognosis in HGSC (30). In addition, a trend towards a positive correlation between granzyme B+ cells and PFS in both post-NACT (30) and treatment naïve (19) OC tumors has been reported.

Here CD4+ or FoxP3+ TILs were not correlated with prognosis. The previous data has been also contradictory with respect to CD4+ TILs and prognosis (19,22). The previous results concerning the prognostic impact of FoxP3+ T cells are also variable (18,19,24,28-30). One explanation is that although FoxP3+ TILs are considered immunosuppressive, FoxP3+ TIL density has

been found to be highly correlated with other TIL densities, possibly reflecting a strong overall T-cell mediated immune response (19). CD68+ TAM density had no correlation with prognosis in our study. Similarly, various previous studies (19,21,32-34) confirmed no correlation between CD68+ TAMs and OC prognosis. We report here that CD163+ TAMs (M2) were correlated with longer PFS. When analyzing multiple histologic types of OC, CD163+ macrophages have been associated with worse prognosis (33,34). However, in two studies with only HGSC patients, controversially, CD163+ TAMs associated with neutral (20) or even favorable (21) prognosis. Although current consensus is that M2 TAMs are immunosuppressive and promote cancer progression (31), the characterization of macrophages into M1 and M2 types may be excessively simplified (21).

The results concerning post-NACT samples should be interpreted with caution since the samples are not sequential, and the number of samples was small. However, WSI and DIA methodology confers reliability and the results should not be therefore omitted. We show here that FoxP3+ cell density was significantly smaller in post-NACT samples compared to treatment naïve specimens. The densities of CD4+ and granzyme B+ TILs were considerably smaller in post-NACT samples, as well, but the statistical power was insufficient to show statistical significance. In two separate studies with paired HGSC tumor samples, the density of FoxP3+ TILs remained unchanged after NACT, while an increase in CD8+ and CD3+ TILs (37), or CD8+, CD4+ and granzyme B+ TILs (30) was observed. In an analysis of unpaired HGSC samples, a decrease in CD3+ sTILs and a trend toward higher ieTIL density post-NACT was observed (20). Overall, due to methodological differences (paired or unpaired samples, different antibodies and scoring systems, whole-slide imaging or tumor-array technology with tumor punches, different histological subgroups) the results concerning the effects of chemotherapy on TME have been very diverse and high individual variation between patients has been shown (20,25,30,36,37). There has been also discussion whether a true comparison between pre- and post-NACT tumors can be performed, since the tumor content or morphology changes tremendously after chemotherapy (42). However, NACT can alter TME and therefore potentially affect the response to both conventional chemotherapy and immune-oncological therapies. Here we show changes

that can be interpreted as both boosting immunity and silencing it and therefore the changes on TME induced by NACT represents an important subject of future studies. Overall, the immune cell counts in post-NACT samples tended to be smaller than in treatment naïve specimens. Additionally, NACT and IDS were correlated with shorter PFS and OS when compared to PDS and adjuvant chemotherapy, possibly reflecting to that NACT is administered to patients having an advanced, inoperable disease.

A strength of the present study is the homogeneity of the patient cohort: all patients had a high-grade carcinoma. Almost all (96 %) patients had HGSC and 90 % presented with an advanced stage disease. In various previous studies, multiple histological subtypes have been analyzed. As grade 2 tumors were previously considered as high grade, in some studies with mostly or exclusively HGSC patients the patient cohort has consisted with both grade 2 and 3 tumors, enhancing the heterogeneity.

The use of WSI and DIA increased the accuracy and reliability of the results. Using QuPath (40) and ImageJ (41) softwares, it was possible to scroll the WSI and compare exact cell counts (CD4+, CD8+, FoxP3+ and granzyme B+) and percentages of positively stained areas (CD68+, CD163+) rather than use a semi-quantitative scale for estimating the cell counts or the extent of the staining. The use of DIA has been shown to increase the accuracy of the assessment when compared with the use of a semi-quantitative scale (38,39). To our knowledge, this report is one of the few studies using WSI and DIA in a cohort of HGSC in assessment of TME content. Additionally, methods presented in this study could be applicable for clinical diagnostics.

Our study has also limitations. First, the patient cohort was rather small (n=67). The number of optimally resected patients was small, as well (n=16). These features may have affected our results. Previously, a correlation between improved outcome and CD8+ (25) or FoxP3+ (19) TILs or CD163+ TAMs (21) has been observed only in optimally debulked patients in some studies. Thus, the low R0 rate of the present study may have had an impact on the results. The small number of post-NACT samples (n=7) made the statistical analyses of this group challenging. Paired pre- and post-NACT specimens were not available, and therefore it was not possible to compare

the changes in the immune cell counts pre- and post-NACT on the same patient.

Another limitation is that the archived FFPE samples were analyzed retrospectively. The patients were operated on and the samples collected during a long period of time (2001–2013). Some of the FFPE samples had to be excluded from analysis due to poor quality, which is at least partially due to long period of conservation. The treatment regimen, FIGO staging classification and the criteria for optimal cytoreduction were changed during the period when the patients were treated. During the recruitment period of the study cohort, the BRCA1/2 mutation analysis was not part of the standard of care and therefore the BRCA1/2 mutation status was not available in most cases. This should be considered when interpreting the results since mutation status represents a major prognostic factor in OC.

In addition, multiplex IHC stainings on the same specimen were not available and therefore it was not possible to study the different immune cell counts or their ratios within the same region of the tumor tissue.

6 CONCLUSIONS

Co-expression of CD8+ and granzyme B+ in TME was correlated with a better prognosis in HGSC, possibly by representing an activated state of immune system and therefore an enhanced anti-tumor immune response in the TME. NACT may affect the immune cell content in the TME and consequently the effect of immuno-oncologic treatments, as well. Further validation studies are needed in larger, prospective OC cohorts for assessment of clinical and especially the predictive significance of combined CD8 and granzyme B positivity as well as the effects of NACT on TME with WSI and DIA.

7 DECLARATIONS

7.1 Acknowledgements

The authors would like to thank Sari Toivola (senior laboratory technician) for conducting the IHC stainings, Reija Autio (Dr. Tech.) for counselling with statistical analyses and Anu Aalto (MD), Seppo Varpuluoma (MD) and Olga Veijalainen (MD) for providing clinical data of patients whose clinical follow-up was organized in regional hospitals. The authors acknowledge the Biocenter Finland (BF) and Tampere Imaging Faculty (TIF) for their service.

7.2 Declaration of Conflicting Interests

The authors declare that there is no conflict of interest.

7.3 Funding

The authors disclosed receipt of the following financial support for the research, authorship and publication of this article: This work was supported by the Competitive State Research Financing of the Expert Responsibility area of Tampere University Hospital and by Relander Foundation, Lahti, Finland.

7.4 Ethical approval

This study has been conducted according to the World Medical Association Declaration of Helsinki and conforms to the ICMJE Recommendations for the Conduct, Reporting, Editing, and Publication of Scholarly Work in Medical Journals. The study protocols have been approved by the Regional Ethics Committee of the Expert Responsibility area of Tampere University Hospital (identification codes: ETL-R09108 and ETL-R11137) for the study. All the study patients have provided a signed informed consent.

7.5 Guarantor

The authors serve as guarantors of this study.

7.6 Contributorship

TJ has contributed to collecting the clinical data, analyzing the IHC stainings, executing the statistical analyses and drafting the manuscript; SL to planning and supervising the study, scanning and analyzing the IHC stainings, planning and interpreting the statistical analyses and drafting and revising the manuscript; JM to revising and commenting the manuscript and SS to planning and supervising the study, planning and interpreting the statistical analyses and drafting and revising the manuscript.

REFERENCES

1. Bray F, Ferlay J, Soerjomataram I, *et al.* Global cancer statistics 2018: GLOBOCAN estimates of incidence and mortality worldwide for 36 cancers in 185 countries. *CA Cancer J Clin* 2018;68(6):394-424.

2. Lheureux S, Gourley C, Vergote I, *et al*. Epithelial ovarian cancer. *Lancet* 2019;393(10177):1240-53.

3. Reid BM, Permuth JB, Sellers TA. Epidemiology of ovarian cancer: a review. *Cancer Biol Med* 2017;14(1):9-32.

4. Berek JS, Kehoe ST, Kumar L, *et al.* Cancer of the ovary, fallopian tube, and peritoneum. *Int J Gynecol Obstet* 2018;143:Suppl 2:59-78.

5. Perren TJ, Swart AM, Pfisterer J, *et al*. A Phase 3 Trial of Bevacizumab in Ovarian Cancer. *New Engl J Med* 2011;365(26):2484-96.

6. Burger RA, Brady MF, Bookman MA, et al. Incorporation of Bevacizumab in the Primary Treatment of Ovarian Cancer. *New Engl J Med* 2011;365:2473-83.

7. Vergote I, Tropé C, Amant F, et al. Neoadjuvant chemotherapy or primary surgery in stage IIIC or IV ovarian cancer. *New Engl J Med* 2010;363:943-53.

8. Kehoe S, Hook J, Nankivell M, et al. Primary chemotherapy versus primary surgery for newly diagnosed advanced ovarian cancer (CHORUS): an open-label, randomised, controlled, non-inferiority trial. *Lancet* 2015: 386(9990);249-57.

9. Moore K, Colombo N, Scambia G, et al. Maintenance Olaparib in Patients with Newly Diagnosed Advanced Ovarian Cancer. *N Engl J Med* 2018;379(26):2495-505.

10. González-Martín A, Pothuri B, Vergote I, et al. Niraparib in Patients with Newly Diagnosed Advanced Ovarian Cancer. *New Engl J Med* 2019;381(25):2391-402.

11. Ray-Coquard I, Pautier P, Pignata S, et al. Olaparib plus Bevacizumab as First-Line Maintenance in Ovarian Cancer. *New Engl J Med* 2019;381(25):2416-28.

12. Gaillard SL, Secord AA, Monk B. The role of immune checkpoint inhibition in the treatment of ovarian cancer. *Gynecol Oncol Res Pract* 2016;3:11.

13. Turner TB, Buchsbaum DJ, Straughn JM, et al. Ovarian cancer and the immune system — The role of targeted therapies. *Gynecol Oncol* 2016;142(2):349-56.

14. Drakes ML, Stiff PJ. Regulation of Ovarian Cancer Prognosis by Immune Cells in the Tumor Microenvironment. *Cancers (Basel)* 2018;10(9):302.

15. Santoiemma PP, Powell DJ. Tumor infiltrating lymphocytes in ovarian cancer. *Cancer Biol Ther* 2015; 16(6):807-20.

16. Zhang L, Conejo-Garcia JR, Katsaros D, et al. Intratumoral T Cells, Recurrence, and Survival in Epithelial Ovarian Cancer. *New Engl J Med* 2003;348(3):203-13.

17. Hwang W, Adams SF, Tahirovic E, et al. Prognostic significance of tumor-infiltrating T cells in ovarian cancer: A meta-analysis. *Gynecol Oncol* 2012;124(2):192-8.

18. Li J, Wang J, Chen R, et al. The prognostic value of tumor-infiltrating T lymphocytes in ovarian cancer *Oncotarget* 2017;8(9):15621–15631.

19. Milne K, Köbel M, Kalloger SE, et al. Systematic Analysis of Immune Infiltrates in High-Grade Serous Ovarian Cancer Reveals CD20, FoxP3 and TIA-1 as Positive Prognostic Factors. *PloS one* 2009;4(7):e6412.

20. van Baal, J O A M, Lok CAR, Jordanova ES, et al. The effect of the peritoneal tumor microenvironment on invasion of peritoneal metastases of high-grade serous ovarian cancer and the impact of NEOADJUVANT chemotherapy. *Virchows Arch*. Epub ahead of print 16 March 2020. DOI: 10.1007/s00428-020-02795-8.

21. Martin de la Fuente, L, Westbom-Fremer S, Skovberg Arildsen N, et al. PD-1/PD-L1 expression and tumor-infiltrating lymphocytes are prognostically favorable in advanced high-grade serous ovarian carcinoma.*Virchows Arch.* Epub ahead of print 24 January 2020. DOI: 10.1007/s00428-020-02751-6.

22. Pinto MP, Balmaceda C, Bravo ML, et al. Patient inflammatory status and CD4+/CD8+ intraepithelial tumor lymphocyte infiltration are predictors of outcomes in high-grade serous ovarian cancer. *Gynecol Oncol* 2018;151(1):10-7.

23. Goode EL, Block MS, Kalli KR, et al. Dose-Response Relationship of CD8+ Tumor Infiltrating Lymphocytes and Survival Time in High-Grade Serous Ovarian Cancer. *JAMA oncol* 2017;3(12):e173290.

24. Hermans C, Anz D, Engel J, et al. Analysis of FoxP3+ T-Regulatory Cells and CD8+T-Cells in Ovarian Carcinoma: Location and Tumor Infiltration Patterns Are Key Prognostic Markers. *PloS one* 2014;9(11):e111757.

25. Wouters MCA, Komdeur FL, Workel HH, et al. Treatment Regimen, Surgical Outcome, and T-cell Differentiation Influence Prognostic Benefit of Tumor-Infiltrating Lymphocytes in High-Grade Serous Ovarian Cancer. *Clinical Cancer Res* 2016;22 (3):714-24.

26. Wang Q, Lou W, Di W, et al. Prognostic value of tumor PD-L1 expression combined with CD8. *Int immunopharmacol* 2017;52:7-14.

27. Rousalova I, Krepela E. Granzyme B-induced apoptosis in cancer cells and its regulation (review). *Int J Oncol* 2010;37(6):1361-78.

28. Zhu Q, Wu X, Wu Y, et al. Interaction between Treg cells and tumor-associated macrophages in the tumor microenvironment of epithelial ovarian cancer. *Oncol Rep* 2016;36(6):3472-8.

29. Shang B, Liu Y, Jiang S, et al. Prognostic value of tumor-infiltrating FoxP3+ regulatory T cells in cancers: a systematic review and meta-analysis. *Sci Rep* 2015;5:15179.

30. Pölcher M, Braun M, Friedrichs N, et al. Foxp3+ cell infiltration and granzyme B+/Foxp3+ cell ratio are associated with outcome in neoadjuvant chemotherapy-treated ovarian carcinoma. *Cancer Immunol Immunother* 2010;59(6):909-19.

31. Cheng H, Wang Z, Fu L, et al. Macrophage Polarization in the Development and Progression of Ovarian Cancers: An Overview. *Front Oncol* 2019;9:421.

32. Ojalvo LS, Thompson ED, Wang T, et al. Tumor-associated macrophages and the tumor immune microenvironment of primary and recurrent epithelial ovarian cancer. *Hum Pathol* 2018;74:135-47.

33. Lan C, Huang X, Lin S, et al. Expression of M2-Polarized Macrophages is Associated with Poor Prognosis for Advanced Epithelial Ovarian Cancer. *Technol Cancer Res Treat* 2013;12(3):259-67.

34. Yuan X, Zhang J, Li D, et al. Prognostic significance of tumor-associated macrophages in ovarian cancer: A meta-analysis. *Gynecol Oncol* 2017;147(1):181-7.

35. Khairallah AS, Genestie C, Auguste A, et al. Impact of neoadjuvant chemotherapy on the immune microenvironment in advanced epithelial ovarian cancer: Prognostic and therapeutic implications. *Int J Cancer* 2018;143(1):8-15.

36. Mesnage SJL, Auguste A, Genestie C, et al. Neoadjuvant chemotherapy (NACT) increases immune infiltration and programmed death-ligand 1 (PD-L1) expression in epithelial ovarian cancer (EOC). *Ann Oncol* 2017;28(3):651.

37. Lo CS, Sanii S, Kroeger DR, et al. Neoadjuvant Chemotherapy of Ovarian Cancer Results in Three Patterns of Tumor-Infiltrating Lymphocyte Response with Distinct Implications for Immunotherapy. *Clinical Cancer Res* 2017;23(4):925-34.

38. Pell R, Oien K, Robinson M, et al. The use of digital pathology and image analysis in clinical trials. *J Pathol Clin Res* 2019; 5(2):81-90.

39. Väyrynen J, Vornanen J, Sajanti S, et al. An improved image analysis method for cell counting lends credibility to the prognostic significance of T cells in colorectal cancer. *Virchows Arch* 2012;460(5):455-65.

40. Bankhead P, Loughrey MB, Fernández JA, et al. QuPath: Open source software for digital pathology image analysis. *Sci Rep* 2017;7(1):16878.

41. Schneider CA, Rasband WS, Eliceiri KW. NIH Image to ImageJ: 25 years of image analysis. *Nat Methods* 2012;9(7):671-5.

42. McCluggage WG, Lyness RW, Atkinson RJ, et al. Morphological effects of chemotherapy on ovarian carcinoma. *J Clin Pathol* 2002;55(1):27-31.